Chemical Physics Letters 807 (2022) 140064

Contents lists available at ScienceDirect

Chemical Physics Letters

journal homepage: www.elsevier.com/locate/cplett

Photodissociation dynamics of xylene isomers $C_6H_4(CH_3)_2$ at 157 nm using an ultracompact velocity map imaging spectrometer – The C_7H_7 channel

Dababrata Paul [a], Zhenghai Yang [a], Arthur G. Suits [b], David H. Parker [c], Ralf I. Kaiser [a,*]

[a] Department of Chemistry, University of Hawai'i at Manoa, Honolulu, HI 96822, United States
[b] Department of Chemistry, University of Missouri, Columbia MO 65211, United States
[c] Department of Laser Physics, Institute for Molecules and Materials, Radboud University, Nijmegen, The Netherlands

ARTICLE INFO

Keywords:
Photodissociation dynamics
Xylene
Tolyl radical
Ultracompact velocity map imaging spectrometer
Vacuum ultraviolet

ABSTRACT

We investigated the photodissociation dynamics of three xylene isomers $C_6H_4(CH_3)_2$ at 157 nm. The center-of-mass translational energy distributions of C_7H_7 radicals were found to peak at 26 kJ mol^{-1}. Although the ionization energy of the C_7H_7 tolyl fragment exceeds the energy of a 157 nm photon, $C_7H_7^+$ was observed as a result of the photoionization of vibrationally 'hot' tolyl (C_7H_7) radicals and/or two-photon ionization. The formation of rovibrationally excited tolyl fragments was discussed. Our experiments suggest the presence of tolyl radicals in the interstellar medium as a precursor to methylated polycyclic aromatic hydrocarbons upon reaction with vinylacetylene (C_4H_4).

1. Introduction

Aromatic volatile organic compounds (VOCs) such as benzene (C_6H_6), toluene ($C_6H_5CH_3$), and xylenes ($C_6H_4(CH_3)_2$) are widely used in household and industrial productions as solvents and raw materials in the production of paint, rubber, plastics, adhesives, irrigation systems, and as gasoline additives to improve anti-knocking properties of aviation fuel [1,2]. The extensive use along with their volatility contributes significant quantities to the pollution of air and aquatic environments, which in turn exerts chronic to acute health effects [1,3]. In addition, VOCs play a significant role in the formation of secondary organic aerosol (SOA) via photo-oxidation [4] and in the gas-phase synthesis of derivatives of polycyclic aromatic hydrocarbons (PAHs) – organic molecules carrying fused benzene rings - such as anions, cations, and alkyl-substituted PAHs in the combustion of fossil fuel [5,6] as well as in the interstellar medium (ISM) [7]. On Earth, PAHs enter the environment from both natural sources and anthropogenic activities and are considered as air pollutants with detrimental effects to human health [8]. Here, PAHs are formed through incomplete combustion of fossil fuel [9] through molecular building blocks facilitating molecular mass growth processes to complex PAHs in flames and in combustion systems [10,11]. Whereas in terrestrial settings, PAHs are considered as unwanted byproducts of an incomplete combustion, PAHs and their derivatives account for up to 20% of the total cosmic carbon budget [12] with the simplest building block – benzene (C_6H_6) - detected in the carbon-rich Westbrook Nebula (CRL 618) [13] and SPM LCM 11 [14–17]. PAHs with 50 carbon atoms and beyond have been linked to unidentified infrared (UIR) emission features in the wavelength region from 3 to 20 μm [18–20] and are presumed to be the carriers of the diffuse interstellar bands (DIBs) [21] in the wavelength range from the visible (400 nm) to the near-infrared (1.2 μm). Besides, infrared bands with the characteristic emission features linked to the aromatic C-H stretching modes at 3.3 μm have been detected in the emission spectra of benzene, naphthalene, phenanthrene, anthracene, and pyrene [20]. Further, the observed 3.4–3.6 μm emission bands have been associated with the C-H stretching modes of the methyl group (CH_3) of methylated PAHs [18,22,23] and have been implicated in molecular mass growth processes transforming a methyl group through reaction with acetylene (C_2H_2) to a five-membered ring annulated to a six-membered ring such as in indene (C_9H_8) [24–26].

Although benzene has been detected in interstellar or circumstellar environments, neither toluene nor xylene isomers have been, although multiple barrier-less reactions to, e.g., toluene have been exposed utilizing crossed molecular beams reactions of, e.g., ethynyl (C_2H) with 1- and 2-methyl-1,3-butadiene (C_5H_8) [27] and the 1-propynyl radical (CH_3CC) with 1,3-butadiene (C_4H_6) [28] opening up pathways to methyl-substituted aromatics not only in cold molecular clouds such as the Taurus Molecular Cloud-1, but also in low temperature,

* Corresponding author.
E-mail address: ralfk@hawaii.edu (R.I. Kaiser).

https://doi.org/10.1016/j.cplett.2022.140064
Received 2 August 2022; Received in revised form 27 August 2022; Accepted 17 September 2022
Available online 23 September 2022

hydrocarbon-rich atmospheres of planets and their moons such as of Titan [29]. However, once formed in the gas-phase, these methyl-substituted aromatics are also subjected to photolysis by the internal vacuum ultraviolet field present even deep inside molecular clouds [9,30] and through the solar photon field interacting with, e.g., Titan's atmosphere. The photodissociation of toluene, the simplest alkyl-substituted benzene, and xylene (o-xylene, m-xylene, and p-xylene) have been investigated in molecular beam experiments. Bersohn et al. reported the dynamics of the hydrogen atom release of toluene and p-xylene at 121.6 nm exploiting laser-induced fluorescence (LIF) detection [31,32]. The methyl (CH_3) elimination channel was also reported as an important dissociation pathway leading to, e.g., the phenyl radical (C_6H_5) as the heavy co-fragment [33–37]. However, a systematic photodissociation study of the photodissociation of o-, m-, and p-xylene and of the methyl elimination channel via carbon–carbon bond rupture leading to distinct C_7H_7 isomers - tolyl, tropyl, and benzyl (Scheme 1) – is still in its infancy [32–35,38]. In this work, we investigate the photodissociation dynamics of three xylene isomers ($C_6H_4(CH_3)_2$) at 157 nm using an ultracompact velocity map imaging spectrometer (UVMIS). The C_7H_7 radicals formed in these processes were detected by photoionization with 157 nm (7.89 eV) photons; further, implications on the dissociation dynamics are presented providing insights into the inherent photodissociation dynamics and isomerization processes on the C_7H_7 potential energy surface (PES).

2. Experimental methods

The ultracompact velocity map imaging spectrometer (UVMIS) for studying photo-dissociation at 157 nm has been described recently elsewhere in detail [39,40]. Briefly, the imaging system consists of a UVMIS lens with a time-of-flight (TOF), a supersonic molecular beam source, and a position-sensitive detector. The UVMIS lens is designed by exploiting multielectrode concepts where five electrodes, i.e., repeller, focusing, extractor 1, extractor 2, and ground are incorporated into an open cylindrical geometry with the dimensions of 20 mm × 20 mm × 35 mm. The voltages of the electrodes were used based on the reference voltage settings with the repeller (1661 V), focusing lens (1316 V), the extractor 1 (472 V), extractor 2 (175 V), and ground. For each photo-dissociation experiment, a pulsed supersonic molecular beam of $C_6H_4(CH_3)_2$ (o-xylene ≥ 97%, m-xylene ≥ 99%, and p-xylene ≥ 99%, Sigma Aldrich) seeded in separate experiments in helium carrier gas (99.9999 %, Airgas) at a level of 0.75 % at a backing pressure of 760 Torr was generated via a pulsed, piezo-crystal driven valve at 10 Hz and 80 μs pulse width. The molecular beam was skimmed and traveled 45 mm to the interaction region; peak velocities of 1288 ± 13 ms^{-1} and speed ratios of 5.3 ± 0.3 were determined. The pressure inside of the main chamber was 2 × 10^{-7} Torr. A vacuum ultraviolet (VUV, 157 nm) laser pulse with a typical energy of 0.62 mJ at 10 Hz was generated by a fluorine (F_2) laser (GAM Ex-10) and was loose focused perpendicularly onto the molecular beam in the interaction region with the help of a lens with a 210 mm focal length. The same VUV laser pulse was used to photodissociate the $C_6H_4(CH_3)_2$ molecule and to subsequently ionize the $C_6H_4CH_3$ radical(s) formed.

The resultant $C_6H_4CH_3^+$ ion cloud was accelerated and focused by the UVMIS system onto a position-sensitive detector composed of a dual-chevron microchannel plate (MCP) and a phosphor screen. The front plate of the MCP was set to zero volts to maintain the field-free region; and a 150 ns high voltage pulse (+2.3 kV) with a bias of + 1.0 kV gate was applied at the second unit to collect the central part of the newton sphere formed by $C_6H_4CH_3^+$ ions, and to separate the signals from background noise originating from, e.g., scattered light. The signals were amplified across the potential developed on MCP plates, and an image was generated on the phosphor screen. A charge coupled device (CCD) camera (IDS, UI-2230SE-M−GL) was placed outside the vacuum chamber to view the phosphor and capturing the image formed on the phosphor screen through a glass window. NuAcq software was used to drive the camera [41], and 15,000 laser shots were accumulated to construct each image. The background was removed from the images by subtracting a background image collected without the molecular beam under otherwise identical experimental conditions.

3. Results and discussion

Fig. 1 (upper panel) shows the raw images of $C_7H_7^+$ (m/z = 91)

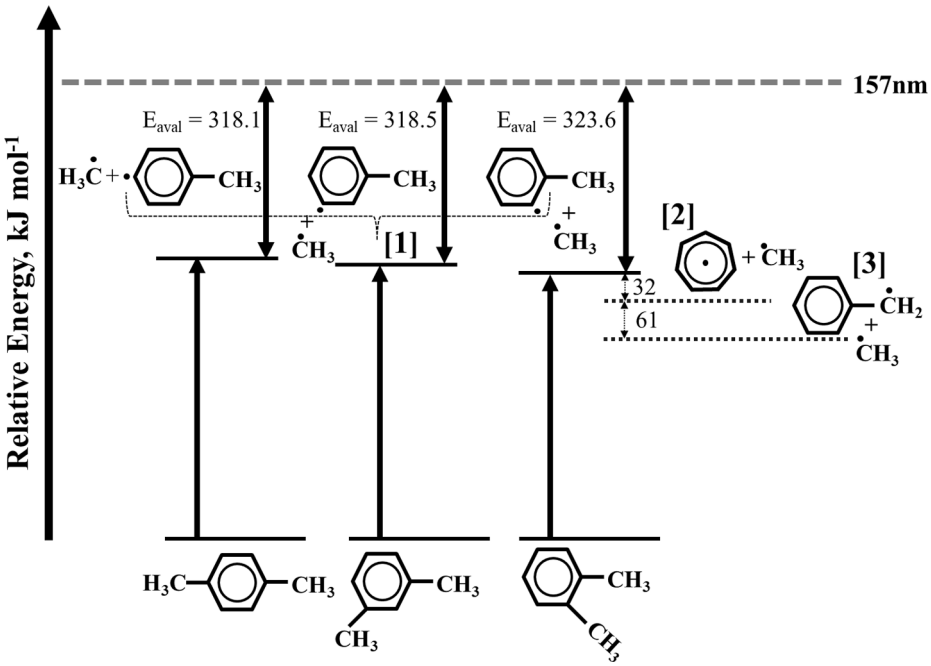

Scheme 1. The energy level diagram for the photodissociation of xylene isomers $C_6H_4(CH_3)_2$ at 157 nm. The relative energies shown are calculated based on the enthalpies of formation of each species at standard conditions from reference [43,44]. The possible isomers of the C_7H_7 radicals are: [1] tolyl radicals, [2] tropyl radicals, and [3] benzyl radicals.

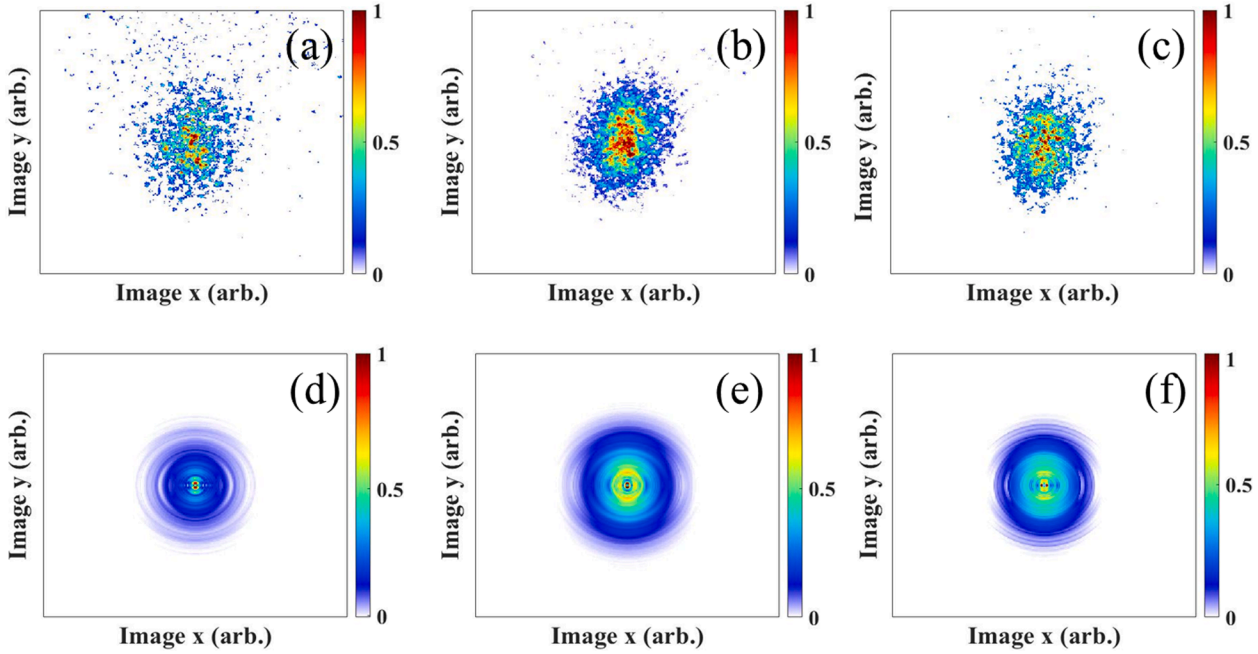

Fig. 1. Raw (upper) and reconstructed (lower) images of $C_7H_7^+$ ($m/z = 91$) from the photodissociation of three xylene isomers $C_6H_4(CH_3)_2$ at 157 nm. The images (a) and (d) are for o-xylene, (b) and (e) for m-xylene, and (c) and (f) for p-xylene, respectively.

resulting from the photolysis of $C_6H_4(CH_3)_2$ isomers at 157 nm. The two-dimensional (2D) raw images are the projection of a Newton sphere formed in the interaction region. The total translational energy distributions are obtained from the velocity distribution by $E_T = \frac{1}{2}\frac{m_{C7H7}}{m_{CH3}}(m_{C7H7} + m_{CH3})v^2_{C7H7}$ at the center-of-mass through a sharp slice, 1 (lower panel), by using FINA software in the "FinaFit" mode [42]. Each translational energy distribution of the $C_7H_7^+$ ions is treated separately with the co-product and displayed in Fig. 2. The center-of-mass translational energy distributions of the C_7H_7 radicals were found to peak at 26 kJ mol^{-1}.

The available energy of each molecular system has been calculated by the energy balance via $E_{aval} = E_{h\nu} - D_0 + E_{int}$, where $E_{h\nu}$, D_0, and E_{int} represent the photon energy, the dissociation energy of the C-C bond, and the internal energy of the parent molecules, respectively. The C-C bond dissociation energies of all three systems are determined based on the enthalpies of formation of each species at standard conditions [43,44]. The internal energies of the parent molecules are assumed to be zero as they are expanded under supersonic molecular beam conditions. The detailed energy partitioning of each system is displayed in Scheme 1.

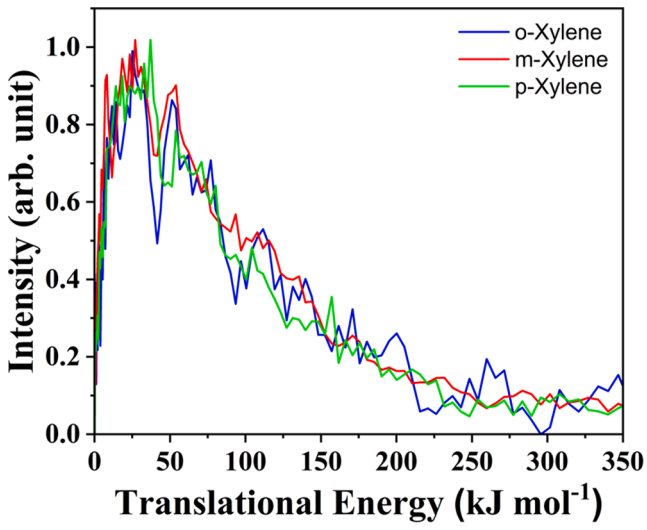

Fig. 2. Center-of-mass translational energy distributions extracted from the $C_7H_7^+$ ion ($m/z = 91$) from the photodissociation of three xylene isomers $C_6H_4(CH_3)_2$ at 157 nm. The relative signal intensity of each system was obtained by integrating three-dimensional (3D) velocity distributions of their corresponding images in Fig. 1.

The gas phase VUV absorption spectra of the xylene isomers (Fig. S1) are similar in shape and show three characteristic features; one intense sharp peak with a maximum absorption (λ_{max}) at 187 nm and two diffuse bands on either side of it in the wavelength region from 145 to 225 nm. Xylene isomers contain two methyl groups on the aromatic benzene ring that might change the λ_{max} value by at least 10 nm to the red shift compared to benzene ($\lambda_{max} = 178$ nm). Compared with the electronic energy level of benzene, the observed absorption peak at $\lambda_{max} = 188$ nm is responsible for the symmetry-allowed $^1A_{1g} \rightarrow {}^1E_{1u}$ transition of the xylene isomers [45]. A shoulder on high energy with the wavelength region 155 to 165 nm implies that states other than the $^1A_{1g} \rightarrow {}^1E_{1u}$ transition are dominant at 157 nm. It is noted that the ionization energies of the xylene isomers vary from 8.44 eV for p-xylene to 8.56 eV for o/m-xylene; these values are very close to the tail of the shoulder of the VUV absorption spectra and separated by 0.5 eV only. Considering the energy difference and converging nature of the shoulder tail to the ionization thresholds, this band might be responsible for Rydberg transitions.

The energetically accessible C-C and C-H bond dissociation pathways lead to the formation of C_7H_7 and C_8H_9 radicals as heavy fragments with the co-products CH_3 and H, respectively. In this letter, we discuss the formation of the C_7H_7 channel. Fig. 2 shows the translational energy distributions of the $C_7H_7^+$ ions derived from the C-C bond dissociation of three xylene isomers $C_6H_4(CH_3)_2$. The center-of-mass translational energy distributions of the C_7H_7 radicals are identical, revealing a maximum translational energy release of about 275 kJ mol^{-1}. Since xylene molecules are populated to the Rydberg state upon 157 nm excitation, it might be argued that the $C_7H_7^+$ ions could be formed via ground state dissociation of the $C_6H_4(CH_3)_2^+$ ions through two-photon absorption process. In that case, the maximum kinetic energy release should be around 400 kJ mol^{-1} [46]. However, no signifying features

emerged in this high-energy region. The maximum kinetic energy release of about 275 kJ mol^{-1} is smaller than the aforementioned value of 400 kJ mol^{-1}, and this value is even lower than the available energies of individual channels formed via C-C rupture, varying from 318.1 kJ mol^{-1} for p-tolyl via 318.5 kJ mol^{-1} for m-tolyl to 323.6 kJ mol^{-1} for o-tolyl derived from the single photon photodissociation process (Scheme 1). It is important to note that the adiabatic ionization energies of the tolyl radicals (C_7H_7) are 7.95 eV for o-tolyl via 8.00 eV for m-tolyl to 8.05 eV for p-tolyl (Scheme 2); these are higher than the energy of the 157 nm photon of 7.89 eV [47]. Therefore, rovibrationally cold nascent tolyl radicals should not be photoionized by a 157 nm photon. Internally 'hot' radicals either rearrange to the radical of lower ionization energy, e.g. tropyl (IE: 6.28 eV) and/or benzyl (IE: 7.24 eV), or contain sufficient internal energy to access the ionization threshold during the ionization process in a single photon ionization of C_7H_7 fragments.

The barrier height for the o-tolyl to benzyl isomerization via hydrogen atom shift was calculated to be 179 kJ mol^{-1} [48]. Considering the energy level diagram, the available energy of 323 for o-tolyl is sufficient to open up the isomerization for benzyl formation. However, the hydrogen shift from the m-tolyl and p-tolyl to the benzyl radical is less favored as wide-reaching bending of the methyl group is necessary to overcome the barrier of the transition state. Alternatively, isomerization to o-tolyl is followed by hydrogen migration to form the benzyl radical, which can then be photoionized. The isomerization has a barrier height of 260 kJ mol^{-1}, which is smaller than the available energy of two systems, e.g. m-tolyl and p-tolyl (318 kJ mol^{-1}) [48]. Taking into account the energy barriers, the hydrogen migration (260 kJ mol^{-1}) would be less favored than the hydrogen migration of o-tolyl to the benzyl radical (179 kJ mol^{-1}). Thus, isomerization would be a slow step in the formation of the benzyl radical, particularly from m-tolyl and p-tolyl. The rate constants for isomerization (m-tolyl and p-tolyl to o-tolyl) and H-migration (o-tolyl to benzyl radical) were estimated to be $< 10^3$ s^{-1} and 10^5 s^{-1}, respectively [48]. The rate constant of benzyl radical formation is 100 faster than the rate constant for isomerization between the tolyl radicals, considering the laser pulse width of 5–20 ns. Note that photoisomerization followed by dissociation and photoionization may be another possible route in the formation of $C_7H_7^+$ ($m/z = 91$) ions. In this pathway, the isomerization of parent xylene isomers must go through via a seven-membered ring prior to dissociation, forming benzyl radicals which then can be photoionized. The barrier height for the six-membered ring to seven-membered ring was estimated to be 364 kJ mol^{-1} [35]. The formation of the tropyl radical via C-C bond rupture at the formation of the seven-membered ring intermediate and the formation of the benzyl radical followed by C-C bond dissociation are stabilized by 32 kJ mol^{-1} and 93 kJ mol^{-1}, respectively (Scheme 1) [49]. It has been shown that the isomerization from a six-membered ring to a seven-membered ring determines the rate of the formation of tropyl and benzyl radicals. The formation rates of tropyl and benzyl radicals via a seven-membered ring are likely 1.5×10^4 s^{-1} based on the rate constant of the analogue system toluene to cycloheptatriene [36].

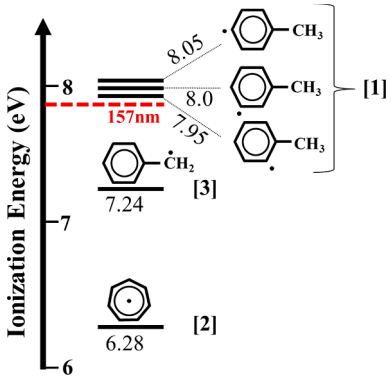

Scheme 2. The ionization energy of the distinct isomers of C_7H_7 radicals: [1] tolyl radical, [2] tropyl radical, and [3] benzyl radical. The red dashed line indicates the energy corresponding to 157 nm.

The average translational energies of the $C_7H_7^+$ ions are nearly identical for the three xylene isomers and are determined to be 61 kJ mol^{-1}. The nearly identical kinetic energy releases resulting from three molecular systems of xylene isomers may suggest a slight decrease in channeling of the total available energy into the internal (rovibrational) degrees of freedom from the o-tolyl via the m-tolyl to the p-tolyl radical during the photodissociation process. Hence, less than 20% of the total available energy is channeled into translational energy. This means that a significant portion of the available energy is directed into the rovibrational excitation of the C_7H_7 radicals. The anisotropy parameter β values were determined for the overall range of velocity distributions of each system and found to be nearly zero, e.g. 0.029 ± 0.002 for m-xylene and 0.004 ± 0.001 for p-xylene. Note that the reliable measurement for o-xylene could not be achieved due to the unwanted background signal in the image. The isotropic angular distribution with less than 20% of the total available energy in translation suggests that the formation of 'hot' tolyl radicals is a consequence of the C-C bond dissociation of parent xylene reactants after internal conversion at the vibrationally excited ground state. The formation of phenyl-type and benzyl-type radicals via C-C and C-H bond dissociations of 'hot' alkylbenzenes (toluene, p-xylene, and mesitylene) at the ground state upon 158 nm irradiation was also reported [50]. It has been shown that the 'hot' p-xylene molecule formed after internal conversion carries 8.03 eV as internal energy. Thus, a large dissipation of energy to the tolyl radical is expected due to the randomization of internal energy prior to bond breaking. However, this simple picture fails to account for the internal energy of the tolyl[1] radicals fragment born in the photodissociation process. This internal energy can result in the single photon ionization of vibrationally 'hot' tolyl radicals. In addition, since the single photon energy is consistent with the transition to the Rydberg states of tolyl radicals, the ionization could be the result of two-photon ionization. Similar observations have also been reported in the photoionization of propyl radicals (n-C_3H_7) upon excitation of n-C_3H_7X (X = CN, OH, HCO) at 157 nm [39].

4. Conclusion

In the present study, we reported the photodissociation of astrophysically relevant xylene isomers $C_6H_4(CH_3)_2$ at 157 nm using an ultracompact velocity map imaging spectrometer (UVMIS). The formation of C_7H_7 radicals via C-C bond dissociation and/or photoisomerization followed by C-C bond dissociation has been investigated based on the pulsed laser photolysis method to shed light on the inherent photodissociation dynamics and isomerization processes. The center-of-mass translational energy distribution of the C_7H_7 radical was found to peak at 26 kJ mol^{-1}. The nearly zero recoil anisotropy with less than 20% of available energy in translation suggests that the formation of 'hot' tolyl radicals is a consequence of direct C-C bond dissociation of parent xylene reactants after internal conversion at the vibrationally excited ground state. Most importantly, although the ionization energy of the C_7H_7 radical formed is higher than the energy of a 157 nm photon, $C_7H_7^+$ was observed in the $C_6H_4(CH_3)_2$ all three xylene isomers as a result of photoionization of vibrationally 'hot' tolyl fragments and/or two-photon ionization. Our experiments suggest the presence of tolyl radicals in the interstellar medium as a precursor to methylated polyreactions with vinylacetylene (C_4H_4).

CRediT authorship contribution statement

Dababrata Paul: Investigation, Data curation, Formal analysis, Visualization, Writing – original draft, Writing – review & editing. **Zhenghai Yang:** Investigation, Data curation. **Arthur G. Suits:** Validation, Supervision. **David H. Parker:** Validation. **Ralf I. Kaiser:**

Conceptualization, Methodology, Writing – original draft, Writing – review & editing, Funding acquisition, Supervision.

Declaration of Competing Interest

The authors declare that they have no known competing financial interests or personal relationships that could have appeared to influence the work reported in this paper.

Acknowledgement

This work was supported by the U.S. Department of Energy, Basic Energy Sciences (Grant No. DE-FG02-03ER15411) to the University of Hawaii at Manoa. AGS acknowledges the DOE under award DE-SC0017130.

Appendix A. Supplementary material

Supplementary data to this article can be found online at https://doi.org/10.1016/j.cplett.2022.140064.

References

[1] E.G. Hancock. Toluene, the xylenes and their industrial derivatives, Elsevier, Amsterdam; New York, 1982.
[2] R.J. Young, R.A. Rinsky, P.F. Infante, J.K. Wagoner, Science 199 (1978) 248.
[3] A. Masih, A.S. Lall, A. Taneja, R. Singhvi, Environ. Pollut. 242 (2018) 1678.
[4] N.L. Ng, J.H. Kroll, A.W.H. Chan, P.S. Chhabra, R.C. Flagan, J.H. Seinfeld, Atmos. Chem. Phys. 7 (2007) 3909.
[5] M. Baroncelli, Q. Mao, S. Galle, N. Hansen, H. Pitsch, Phys. Chem. Chem. Phys. 22 (2020) 4699.
[6] N. Hansen, M. Schenk, K. Moshammer, K. Kohse-Höinghaus, Combust. Flame 180 (2017) 250.
[7] S. Doddipatla, G.R. Galimova, H. Wei, A.M. Thomas, C. He, Z. Yang, A.N. Morozov, C.N. Shingledecker, A.M. Mebel, R.I. Kaiser, Sci. Adv. 7 (2021) eabd4044/1.
[8] K.S. Johnson, B. Zuberi, L.T. Molina, M.J. Molina, M.J. Iedema, J.P. Cowin, D. J. Gaspar, C. Wang, A. Laskin, Atmos. Chem. Phys. 5 (2005) 3033.
[9] R.I. Kaiser, N. Hansen, J. Phys. Chem. A 125 (2021) 3826.
[10] K. Okude, K. Mori, S. Shiino, T. Moriya, SAE trans. 113 (2004) 1002.
[11] M. Frenklach, Phys. Chem. Chem. Phys. 4 (2002) 2028.
[12] A.G.G.M. Tielens, Annu. Rev. Astron. Astrophys. 46 (2008) 289.
[13] J. Cernicharo, A.M. Heras, A.G.G.M. Tielens, J.R. Pardo, F. Herpin, M. Guélin, L.B. F.M. Waters, Astrophys. J. 546 (2001) L123.
[14] C.S. Contreras, F. Salama, Astrophys. J. Suppl. Ser. 208 (2013) 6.
[15] J. Bernard-Salas, E. Peeters, G.C. Sloan, J. Cami, S. Guiles, J.R. Houck, Astrophys. J. 652 (2006) L29.
[16] J.A.D.L. Blommaert, J. Cami, R. Szczerba, M.J. Barlow, Space Sci. Rev. 119 (2005) 215.
[17] M. Frenklach, E.D. Feigelson, Astrophys. J. 341 (1989) 372.
[18] A.G.G.M. Tielens, Rev. Mod. Phys. 85 (2013) 1021.
[19] L.J. Allamandola, D.M. Hudgins, S.A. Sandford, Astrophys. J. 511 (1999) L115.
[20] J. Shan, M. Suton, L.C. Lee, Astrophys. J. 383 (1991) 459.
[21] P.J. Sarre, J.R. Miles, S.M. Scarrott, Science 269 (1995) 674.
[22] E. Peeters, C.W. Bauschlicher, L.J. Allamandola, A.G.G.M. Tielens, A. Ricca, M. G. Wolfire, Astrophys. J. 836 (2017) 198/1.
[23] C.J. Mackie, E. Peeters, C.W. Bauschlicher Jr, J. Cami, Astrophys. J. 799 (2015) 131/1.
[24] A.M. Mebel, A. Landera, R.I. Kaiser, J. Phys. Chem. A 121 (2017) 901.
[25] D.S.N. Parker, R.I. Kaiser, O. Kostko, M. Ahmed, ChemPhysChem 16 (2015) 2091.
[26] R.I. Kaiser, T.L. Nguyen, T.N. Le, A.M. Mebel, Astrophys. J. 561 (2001) 858.
[27] B.B. Dangi, D.S.N. Parker, R.I. Kaiser, A. Jamal, A.M. Mebel, Angew. Chem. Int. Ed. 52 (2013) 7186.
[28] A.M. Thomas, C. He, L. Zhao, G.R. Galimova, A.M. Mebel, R.I. Kaiser, J. Phys. Chem. A 123 (2019) 4104.
[29] R.I. Kaiser, D.S.N. Parker, A.M. Mebel, Annu. Rev. Phys. Chem. 66 (2015) 43.
[30] A. Yabushita, T. Hama, M. Kawasaki, J. Photochem. Photobiol. C: Photochem. Rev. 16 (2013) 46.
[31] J. Park, R. Bersohn, I. Oref, J. Chem. Phys. 93 (1990) 5700.
[32] K. Tsukiyama, R. Bersohn, J. Chem. Phys. 86 (1987) 745.
[33] N.B. Bejoy, M. Kawade, S. Singh, G.N. Patwari, J. Phys. Chem. A 126 (2022) 1960.
[34] S. Mishra, N.B. Bejoy, M. Kawade, H.P. Upadhyaya, G.N. Patwari, J. Chem. Sci. 133 (2021) 128.
[35] C.-L. Huang, J.-C. Jiang, Y.T. Lee, C.-K. Ni, J. Phys. Chem. A 107 (2003) 4019.
[36] C.-K. Lin, C.-L. Huang, J.-C. Jiang, A.H.H. Chang, Y.T. Lee, S.H. Lin, C.-K. Ni, J. Am. Chem. Soc. 124 (2002) 4068.
[37] R. Fröchtenicht, J. Chem. Phys. 102 (1995) 4850.
[38] S. Lange, K. Luther, T. Rech, A.M. Schmoltner, J. Troe, J. Phys. Chem. 98 (1994) 6509.
[39] D. Paul, Z. Yang, S.J. Goettl, A.M. Thomas, C. He, A.G. Suits, D.H. Parker, R.I. Kaiser, J. Phys. Chem. A 126 (2022) 5768.
[40] E. Sakkoula, B.G.M. van Oorschot, D.H. Parker, Mol. Phys. 120 (2022) e1910357/1.
[41] W. Li, S.D. Chambreau, S.A. Lahankar, A.G. Suits, Rev. Sci. Instrum. 76 (2005) 063106/1.
[42] J.O.F. Thompson, C. Amarasinghe, C.D. Foley, A.G. Suits, J. Chem. Phys. 147 (2017), 013913.
[43] T. Yang, L. Muzangwa, R.I. Kaiser, A. Jamal, K. Morokuma, Phys. Chem. Chem. Phys. 17 (2015) 21564.
[44] G. da Silva, C.-C. Chen, J.W. Bozzelli, J. Phys. Chem. A 111 (2007) 8663.
[45] A. Bolovinos, J. Philis, E. Pantos, P. Tsekeris, G. Andritsopoulos, J. Mol. Spectrosc. 94 (1982) 55.
[46] C. Cone, M.J.S. Dewar, D. Landman, J. Am. Chem. Soc. 99 (1977) 372.
[47] T. Bierkandt, P. Hemberger, P. Oßwald, M. Köhler, T. Kasper, Proc. Combust. Inst. 36 (2017) 1223.
[48] E. Dames, H. Wang, Proc. Combust. Inst. 34 (2013) 307.
[49] G. da Silva, J.A. Cole, J.W. Bozzelli, J. Phys. Chem. A 114 (2010) 2275.
[50] T. Shimada, Y. Ojima, N. Nakashima, Y. Izawa, C. Yamanaka, J. Phys. Chem. 96 (1992) 6298.